seemed to occur (Table 1, Fig. 1). This was paired with a forward primer (ZghIGSu1: its 5′ end 6 nt downstream of the 3′ end of primer ZghIGSu). Within the 5′ portion of the IGS, two other primer pairs were designed to amplify shorter portions of the putative variable region (Table 1, Fig. 1). Of these, one pair (IGSF1 and IGSR2) immediately flank the AT-rich region.

To investigate possible variation in the 3′ half of the IGS, a forward primer (IGSd1RC: the reverse complement of ZghIGSd1) was used in conjunction with primer ET10. A single band of about 900 bp was predicted. All PCR products were separated in a 1% agarose gel.

2.5. Sequence analysis

The characteristics of 28S–18S IGS rDNA for *S. japonicum* were initially determined by comparison with previously published IGS rDNA sequences of *Schistosoma haematobium*, *Schistosoma guineensis* (= *Schistosoma intercalatum* in Kane and Rollinson, 1998) and *Schistosoma mansoni* (Kane and Rollinson, 1998). Given that the IGS regions of the first two of these species are very similar, we included only *S. guineensis* and *S. mansoni* in analyses reported here.

BLASTn (Zhang et al., 2000) searches in GenBank identified related sequences from *S. japonicum* in the public databases. In addition, supercontigs produced by the *S. japonicum* genome sequencing effort (*Schistosoma japonicum* Genome Sequencing and Functional Analysis Consortium et al., 2009, and available from http://lifecenter.sgst.cn//cn/schistosomaCnIndexPage.do and http://chgc.sh.cn/japonicum) were searched. The worms used for the genome sequencing project came from a single location in Anhui Province (*Schistosoma japonicum* Genome Sequencing and Functional Analysis Consortium et al., 2009). All relevant sequences were brought into the manual alignment program BioEdit (Hall, 1999) for examination and further analysis.

SelfBLASTn (Altschul et al., 1997) was used to seek direct or inverted repeats in all schistosome species, as were dot-plots (at http://www.vivo.colostate.edu/molkit/dnadot/) and Palindrome available at http://mobyle.pasteur.fr/cgi-bin/portal.py?form=palindrome. Generally, repeats or other features less than 10 bp in length were not considered. We labelled repeats in *S. japonicum* alphabetically following sequentially from the scheme used for African schistosomes (Kane and Rollinson, 1998).

Blast Output Visualization Tool (BOV) (Gollapudi et al., 2008) (http://bioportal.cgb.indiana.edu/cgi-bin/BOV/index.cgi) was used to construct a visual representation of patterns of repeats from all schistosome species. The output files of local BLAST searches were loaded into BOV and diagrammatic representations of repeated motifs, including inverted repeats, were generated. These diagrams were edited to include additional features, and especially direct sub-repeats, that are not always indicated in standard BLAST searches.

The IGS region of *S. japonicum* was compared with those of the cestode *E. granulosus* (U26429) and the monogenean *G. salaris* (AJ276033) using dotplots, pairwise alignments and visual inspections of any regions where similarities were suspected.

3. Results

3.1. Description of a typical IGS in S. japonicum

All sequences generated during this study have been deposited in GenBank (EU835683-EU835706). The length of the longest clone sequenced (EU835692, from Zhejiang Province) is 1838 bp and is our reference sequence. The length of the IGS in this clone, after removal of flanking 28S and 18S sequence, is 1457 bp. The IGS exhibits the following features (Figs. 1 and 2): (1) A 32-nt tract lacking obvious features; (2) 85 nt of sequence rich in AT repeats; (3) a tract of about 400 nt including 9 direct dispersed copies, several somewhat truncated and slightly divergent, of a motif of maximum length 17 nt (repeat J in Figs. 1 and 2); (4) overlapping the 3′ end of the first copy of repeat J by 3 nt is a tract of 11 nucleotides (repeat K), the exact reverse complement of which overlaps the 3′ end of the eighth copy of J; (5) repeat L (11 nt) appears once starting 112 nt downstream of the last direct copy of repeat J and again in reverse complement 12 nt downstream of the reverse complement copy of J; (6) repeat J appears once in reverse complement following a tract of 46 nt of unique sequence downstream of L; (7) the second half of the IGS contains two pairs of short and imperfect repeats, repeat M (12 nt) and repeat N (10 nt).

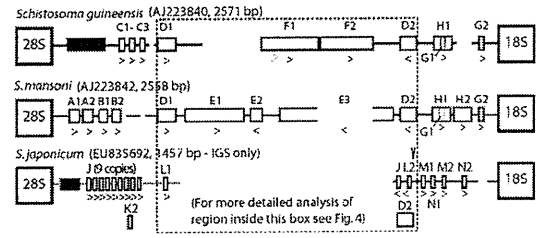

Fig. 2. Schematic diagram (not to scale) of the components of the IGSs for *Schistosoma* species. Information for the African species came from Kane and Rollinson (1998). Repeats are shown as open boxes, with an arrowhead indicating whether each is direct or inverted. Repeats coded by the same letter are identical or similar in sequence. The terminology for repeats extends that of Kane and Rollinson (1998). The AT-rich region (present in *S. guineensis* and *S. japonicum*) is shown as a filled box. Breaks in the horizontal line indicate large alignment gaps. The dotted line in *S. japonicum* indicates sequence that cannot be aligned with that of the African species. The arrowhead close to L2 indicates the putative transcription start point in *S. japonicum*. Lengths given refer to IGS only and do not include flanking regions in 28S and 18S genes.

3.2. Length variants in cloned IGS amplcons

Cloned amplicons from all worms from Sichuan (EU835686-EU835688, EU835693, EU835694, EU835703) and Yunnan (EU835695-EU835698) Provinces yielded IGS sequences with the structure given above. Shorter IGS variants that were sequenced differed in structure from EU835692 only 5′ of repeat L, upstream of which deletions of various lengths were noted. In particular, the AT-rich region was often absent. The samples from Jiangxi (EU835683-EU8356685) additionally lacked the first three copies of J, and K1. Sequences from remaining samples lacked between 141 and 256 nt from the 3′ end of the 28S gene and sometimes one or more of the J repeats. The shortest IGS sequences were from the Yueyanglou District of Hunan Province (EU835701-EU835702). Cloned amplicons from this locality lacked all of the J and K repeats (with the exception of the reverse-complement J repeat).

Although our sequences from cloned PCR products initially suggested a geographical basis for the length variants of the IGS, amplification of the 5′ part of the region revealed many, often identical, bands in every sample regardless of its place of origin (Fig. 3A). One main band of about 1200 bp was evident in all samples. None of our sequenced PCR products corresponded exactly with this length. A less intense band at about 1000 bp in most samples might correspond with the EU835692 (expected to be 952 bp). Many smaller bands were shared by most samples although a few exhibited unique bands. The results depicted in Fig. 3A suggest little or no locality-specific variation, but instead they suggest some intra-individual variation.

Supercontigs from the *S. japonicum* genome project that lacked internal tracts of "N" commonly had an assembled length for the

Please cite this article in press as: Zhao, G.-H., et al., The ribosomal intergenic spacer (IGS) region in *Schistosoma japonicum*: Structure and comparisons with related species. Infect. Genet. Evol. (2011), doi:10.1016/j.meegid.2011.01.015

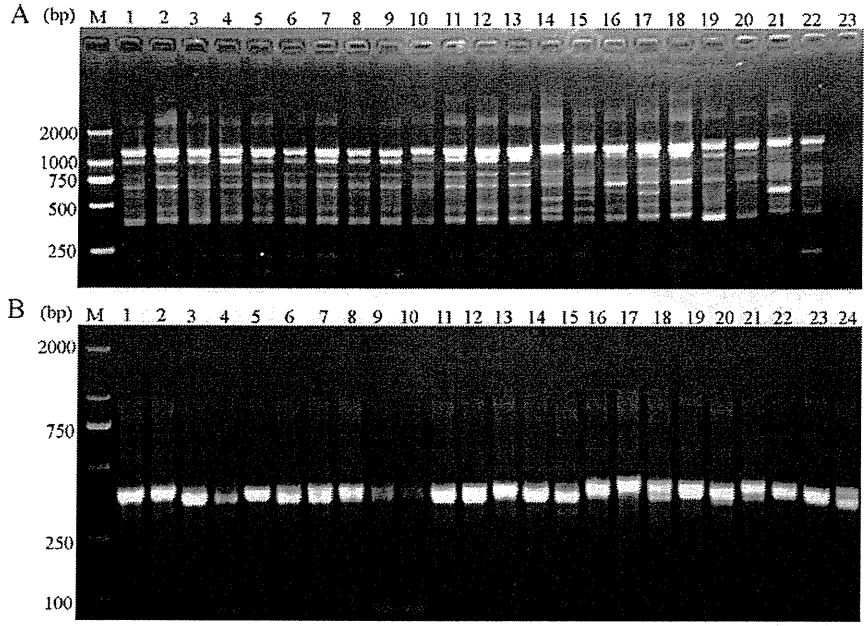

Fig. 3. (A) PCR products amplified by primer pair ZghIGSu1 and ZghIGSd1 for each sample (Table 2 and Fig. 1). It therefore amplifies through the region where the length variation appears to occur. Note one main band of about 1200 bp in all samples. There is a less intense band at about 1000 bp in most samples and smaller bands shared by most samples. A few have unique bands. Lanes 1 and 2 show samples from Zhejiang; lanes Lanes 3 and 4, Jiangxi; lanes 5–11, Sichuan; lanes 12 and 13, Yunnan; lanes 14–20, Hunan, lanes 21 and 22, Anhui; lane 23 negative control. M represents a DNA size marker (ordinate values in bp). (B) Representative PCR products for primer combination IGSF1 and IGSR2. This primer pair amplifies through the AT-rich region and is expected to produce a band of 149 bp based on EU835692. Lanes 1–8 show samples from Sichuan; lanes 9–12, Yunnan; lanes 13 and 14, Zhejiang; lanes 15 and 16, Anhui; lanes 17–22, Hunan; lanes 23 and 24, Jiangxi. Slight length differences and some double bands are apparent. M represents a DNA size marker (ordinate values in bp).

IGS region of 1695 bp. This is over 200 bp longer than our longest sequences, with the length difference being entirely a consequence of a longer AT-repeat region. The length of the 5′ half, which would be amplified by primers ZghIGSu1 and ZghIGSd1, was about 1200 bp in these contigs (e.g. SJC_S012163). This is about the size of the major band in Fig. 3A.

To investigate further the length variation in the 5′ half of the IGS, we designed new forward and reverse primers either side of the AT-rich region. Only PCRs spanning the AT-rich region yielded amplicons longer than expected by comparison with EU835692, the difference being consistently about 250–300 bp. Some intra-individual variation was apparent when primer pair IGSF1 and IGSR2 was used. However this was not very marked (Fig. 3B).

While amplification of the 5′ part of the IGS yielded many bands, amplification of the 3′ portion yielded only a single band from every sample. This was of the expected length of ~900 bp (results not shown), indicating no geographical or intra-individual length variation in this region.

Other than the length variants discussed above, differences between sequences obtained were limited to the occasional point substitution (compare GenBank accessions).

3.3. Beginnings and ends of transcripts

We identified the 3′ end of the 28S gene (Fig. 1) by comparison with other studies, principally Kane and Rollinson (1998). The 3′ end of the full-length rRNA precursor transcript probably lies in the first 10 nt of the IGS, suggesting a very short 3′ ETS. All *S. japonicum* ESTs (e.g. BU802830) in GenBank extending to this point had a poly-A tail starting within 10 nt after the putative 3′ end of the 28S gene.

There is some evidence concerning the location of the start of transcription of the full-length rRNA precursor. One EST from *S. japonicum* is available in GenBank (FN328106) spanning the last 738 nt of the IGS of this species and extending a short distance into the 18S gene. It is possible that the start of this EST represents the start of the 5′ external transcribed spacer (ETS). A putative transcription initiation site (TATATAGGG–as discussed in Kane and Rollinson, 1998) was found largely overlapping the inverted copy of repeat L (thus lying within D2 of the African species and slightly modified in *S. mansoni*). This is exactly where FN328106 starts. No EST from *S. japonicum* matches anything upstream of this. Capowski and Tracy (2003), following Kane and Rollinson (1998), accepted this as also being the transcription start point in *S. mansoni*. Some ESTs from *S. mansoni* start at about this location (e.g. CD133503). However, others start much further upstream of this.

3.4. Comparisons with African species

Comparisons with sequences of African schistosomes were very revealing. Initial impressions were that the 5′ half of the IGS region of *S. japonicum* was very different from that of the African schistosomes (Fig. 2). Closer analysis, however, revealed subtle points of similarity. Repeats B1 and B2 in *S. mansoni* in Fig. 2 of Kane and Rollinson (1998) are misaligned against the sequence of *S. guineensis*. The second half of B2 corresponds with the C repeats in *S. guineensis*, which in turn closely resemble the J repeats in *S. japonicum*. There does not appear to be an inverted copy of C in the African species, whereas an inverted copy of J overlaps the start of D2 in *S. japonicum*. Apart from these features, there is no similarity between the African species and *S. japonicum* 5′ of D1.

The long D1–D2 region contains much of the complexity in the African species, but this region is largely missing from *S. japonicum*. The main features recognised in the D1–D2 region by Kane and Rollinson (1998) in African species are shown in Fig. 2. Apart from the inverted repeats, D1 and D2 which book-end this region, a pair of large direct tandem repeats (F1 and F2) occurs in *S. guineensis*. In

Please cite this article in press as: Zhao, G.-H., et al., The ribosomal intergenic spacer (IGS) region in *Schistosoma japonicum*: Structure and comparisons with related species. Infect. Genet. Evol. (2011), doi:10.1016/j.meegid.2011.01.015

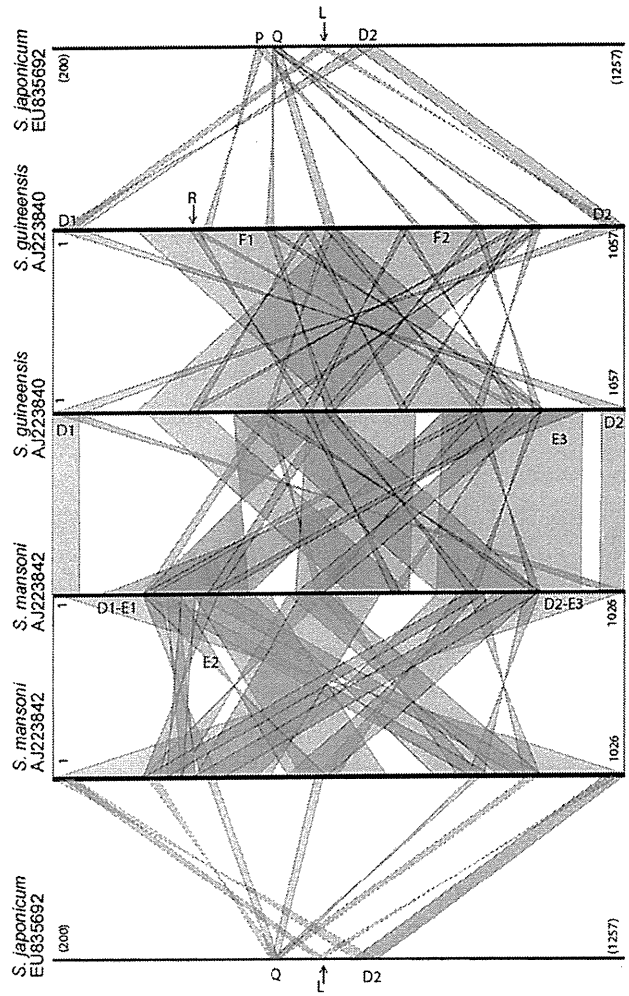

Fig. 4. D1–D2 region (boxed in Fig. 2) of *S. japonicum* and African schistosomes compared. Graphical output from BOV was edited to show additional feature. The thick horizontal lines represent the linear DNA sequence between and including D1 and D2 in the African species. Similar regions in two sequences that are joined by parallel lines are direct repeats. If the lines cross each other, the indicated regions are reverse complements of each other. Dashed lines indicate repeats that were not identified by the BLAST searches and have been manually added. In *S. mansoni*, the D1–D2 region is 1026 bp in length: in *S. guineensis*, it is 1057 bp. Most of the IGS region of *S. japonicum* is included in the figure to facilitate comparison. The putative D1–D2 region in *S. japonicum* is very short and is bounded by L and D2.

S. mansoni, a large tract of sequence, E1, is followed by a reverse-complement of part of this tract (E2) and then by a complete inverted copy (E3). E3 aligns easily with a large portion of repeat F seen in *S. guineensis*. These features are revealed by the more detailed comparisons summarised in Fig. 4. Sequence corresponding to D2 is present in *S. japonicum*. Therefore for comparison in Fig. 4 we included a length of the IGS of this species (positions 200-1257 in EU835692) centred around D2 and of about the same length as the D1–D2 region in the African species. D1 might be represented in *S. japonicum* by motif L1 (TATATAACATG), present slightly upstream of D2 (Figs. 1 and 2), thus making the putative D1–D2 region in *S. japonicum* a mere 113 bp in length, about 10% of the length in the African species. Although F1 and F2 cannot be recognised in *S. japonicum*, a short motif present in this species (P: ATTTTGATAAAAA), and lying upstream of the D1–D2 region, is present in reverse complement at about the middle of F1 and F2 in *S. guineensis* (Fig. 4). Another nearby motif (Q: TCATAACTTTT-GAATGG), present once in *S. japonicum*, is represented once in reverse complement in F1 and in F2 in *S. guineensis*, and also as a direct copy at the 3′ end of F1 and F2. Five copies of this motif, in either orientation, also occur in comparable regions in *S. mansoni* (Fig. 4) although generally as part of longer repeat motifs. Substitutions in *S. mansoni* relative to *S. japonicum* lead to some of these features not being easily recognised in a BLAST search.

In addition to the large direct repeats, F1 and F2, the main features noted in *S. guineensis* are the short repeats, Q, mentioned above. Another motif, R (ATAGAAAGTCCGAG), is present 4 times in *S. guineensis*, twice direct and twice inverted. This motif appears only once in *S. mansoni* and is not present in *S. japonicum*. Comparisons between *S. guineensis* and *S. mansoni* reveal a very complicated pattern of duplications and translocations, some inverted (Fig. 4). In *S. mansoni*, the most conspicuous feature is the large inverted repeat that starts and ends the D1–D2 region and constitutes about two-thirds of the region. This involves D1–E1 at the 5′ end and D2–E3 at the 3′ end. Also conspicuous are the five copies of a motif centred around Q seen in the other *Schistosoma* species, albeit only once in *S. japonicum*.

Beyond the D1–D2 region, sequences of African species align more-or-less readily with those from *S. japonicum* and with very few indels. However, there are few shared interesting features. Repeats M and N in *S. japonicum* are not found in the African species and repeats G and H in the African species do not occur in *S. japonicum*. However, a motif (S: TGATCTTGGTGGT), proposed as a chi-like motif by Kane and Rollinson (1998), occurring once slightly before N2 in *S. japonicum*, aligns with a near-identical copy in the African species here. A slightly variant copy of S occurs in the African species some 260 bp earlier in a region of poor alignment with *S. japonicum*.

Comparisons of IGS sequence data of schistosomes with those of the cestode *E. granulosus* (Picón et al., 1996) and the monogenean *G. salaris* (Collins and Cunningham, 2000) failed to demonstrate any points of similarity.

4. Discussion

4.1. The question of geographical variation in S. japonicum

The question that initially prompted this work is whether or not there is geographical variation in the IGS in *S. japonicum*. The sequences of amplicons reported here suggested that this is the case, with all length differences being in the 5′ half of the region (Fig. 3A). However, amplification of the 5′ half using an internal reverse primer indicated that the major IGS copy might be around 250–300 bp longer than our reference sequence (EU835692) (Fig. 3A and Table 2) in all samples, regardless of geographical origin. Multiple, shorter bands were also apparent for each sample, but these were also mostly similar in length among samples. Indeed, Fig. 3A suggests limited inter-locality variation but some intra-individual variation. To investigate this further, we amplified shorter portions

Table 2
Anticipated and actual PCR product sizes for primer pairs.

Forward	Reverse			
	ET10	ZghIGSd1	IGSR2	IGSR1
ZghIGSu1		952 (see Fig. 3A)	472 (~700[a])	353 (~350[b])
IGSF1		628 (~800[a])	149 (~350[c], see Fig. 3B)	
IGSF2		508 (~500[b])		
IGSd1RC	892 (~900[b])			

Values are anticipated length based on EU835692 and (estimated length of band in an agarose gel). Positions and orientation of primers are shown in Fig. 1.
[a] Single dominant band but not of expected size, see text.
[b] Single band of expected size.
[c] Generally one dominant band per worm, but some length variation and some double bands.

Please cite this article in press as: Zhao, G.-H., et al., The ribosomal intergenic spacer (IGS) region in *Schistosoma japonicum*: Structure and comparisons with related species. Infect. Genet. Evol. (2011), doi:10.1016/j.meegid.2011.01.015

of the 5′ half of the IGS. These also indicated limited inter-locality variation but some individual length variation in the AT-rich region (Fig. 3B). Amplification through the AT-rich region indicated that the length difference between the expected product of primer pair ZghIGSu1 and ZghIGSd1 (952 bp in EU835692) and the dominant band in Fig. 3A (~1200 bp) is entirely due to the AT-rich region. Contigs from the *S. japonicum* genome sequencing project often have a long AT-rich region consistent with this.

None of the PCRs within the 5′ half of the IGS yielded bands consistent with the large deletions noted in some of our cloned and sequenced amplicons. We have to conclude that these deletions are PCR or cloning artifacts. PCR-amplification through repetitive regions can produce misleading results, in particular preferential amplification of shorter copies. Mateos and Markow (2005) found that estimates of IGS lengths in insects obtained by PCR could be very different (usually shorter) than those obtained by Southern blotting. They also noted considerable intra-individual variation, both on the basis of PCR and Southern blotting. We have also detected intra-individual variation in *S. japonicum*, but proper quantification of this must await studies using Southern blotting. Simpson et al. (1984) detected some inter-individual variation in the ribosomal repeats of *S. mansoni*, and reckoned, on the basis of Southern blotting, that 10% of repeats exhibited length variation within an individual. We conclude that geographical variation might exist in *S. japonicum*, but appears to be limited and attempts to demonstrate it using PCR will be confounded by intra-individual variation and PCR artifacts.

4.2. Beginnings and ends of transcripts

We have accepted the 3′ end point of the 28S suggested by Kane and Rollinson (1998). They chose this location largely on the basis of comparison with sequences of 28S genes from other taxa. They also noted the existence of an EST from *S. mansoni* that had a short poly(A) tail commencing at the exact position they accepted as the 3′ end of the 28S gene. We found a similar situation for a number of ESTs from *S. japonicum*, and are tempted to infer that the 3′ end of the primary transcript lies close to this location. RNA polymerase I is not known to produce transcripts with a poly(A) tail. However, the polyadenylation of ribosomal transcripts has been noted and indicates defective or excess transcripts tagged by surveillance processes for degradation and recycling (Lafontaine, 2010). Low levels of normal transcripts are also polyadenylated (Lafontaine, 2010). In the absence of any other information, such ESTs might provide the best hints as to the location of the end of the transcript.

The 3′ half of the IGS of *S. japonicum* aligns readily, and with rather few indels, with homologous regions in African schistosomes (Fig. 1). Indirect evidence, outlined in the Section 3, places the start of transcription at the start of this region of strong similarity.

4.3. Comparisons with African species: identification of phylogenetically conserved motifs

Comparisons of all the schistosome species revealed potentially functional features that would not have been detected by analysis of a single species. Prime among these are the motifs B/C/J and P, Q and S. These are the few shared features common to the three species. Presumably it is these repeated regions that act in the various transcription initiating and promoting roles.

In general, the rDNA promoter is a region of 100–150 bp overlapping the transcription initiation site, but largely upstream of it (Moss and Stefanovsky, 1995). Within this region lies a "core" promoter element (CPE) close to the transcription initiation site and an upstream control element (UCE). Further upstream lie other promoter and enhancer elements. It is reasonable to assume that elements shared by *S. japonicum* and the African schistosomes include important regulatory sequences in the IGS. The reverse-complement of repeat L in *S. japonicum*, present also in D2 in the African species, lies at the putative transcription start site. This element and the portion immediately downstream of it includes the sequence TATATAGGG, proposed by many authors as a likely core promoter (Kane and Rollinson, 1998). If this is so, we should expect to find an upstream control element within about 150 bp. The direct copy of repeat L in *S. japonicum* lies within this range and occurs within D1 in African species. Elements P and Q are a little further upstream but occur multiply within the D1–D2 region in African species. It is likely that these have functional significance. Repeat J in *S. japonicum* is also present as elements B and C in *S. mansoni* and *S. guineensis*, respectively. There are more copies in *S. japonicum* than in the African species, and a reverse-complement of the element is not seen in African species. That these have a functional role is likely.

It is known that IGS regions can diverge rapidly, even between related species (Ambrose and Crease, 2010). Recent estimates place the divergence between *S. japonicum* and African species in the mid-Miocene (Snyder and Loker, 2000; Morgan et al., 2003; Lockyer et al., 2003; Attwood et al., 2007). According to theories developed by these authors, *Schistosoma* arose in central Asia, probably parasitizing murids, and early species subsequently dispersed to Africa at the time of a faunal interchange between the two regions. An estimate for the split at 15–20 MYA is therefore reasonable. At first glance, the IGS region of *S. japonicum* upstream of the putative transcription start site has little similarity with those of the African schistosomes, consistent with the high rate of evolution in this region. However, our analyses have identified a number of elements conserved across this span of time. Some of these, such as the reverse complement of L, are identical with promoters proposed in other studies. Such conserved elements should be the focus of future investigation. The bewildering array of repeats, nested and overlapping, reversed and direct, seen in the large D1–D2 region of African schistosomes is very short and simple in *S. japonicum*. Lack of phylogenetic conservation suggests the complex African version it is not essential for successful transcription of the ribosomal genes.

In conclusion, we failed to confirm the existence of population-level variation in the IGS region of *S. japonicum*, although this has to be checked by additional studies and the use of Southern blots. Our comparisons of the IGS sequence with those of African schistosomes revealed a number of sequence elements of presumed functional significance that have been conserved since the divergence of the species.

Acknowledgements

Project support was provided in part by the National Basic Research Program (973 program) of China (grant no. 2007CB513104), The State Key Laboratory of Veterinary Etiological Biology, Lanzhou Veterinary Research Institute, CAAS, the Yunnan Provincial Program for Introducing High-level Scientists (grant no. 2009CI125), the Program for Changjiang Scholars and Innovative Research Team in University (grant no. IRT0723) to XQZ, the Special Funds for Talents in Northwest A & F University to GHZ, and the National Natural Science Foundation of China (grant no. 30960280) to FCZ. Professor Baozhen Qian of Bioengineering Institute, Zhejiang Academy of Medical Sciences, China was thanked for providing some *S. japonicum* samples used in the present study.

References

Altschul, S.F., Madden, T.L., Schäffer, A.A., Zhang, J., Zhang, Z., Miller, W., Lipman, D.J., 1997. Gapped BLAST and PSI-BLAST: a new generation of protein database search programs. Nucleic Acids Res. 25, 3389–3402.

Please cite this article in press as: Zhao, G.-H., et al., The ribosomal intergenic spacer (IGS) region in *Schistosoma japonicum*: Structure and comparisons with related species. Infect. Genet. Evol. (2011), doi:10.1016/j.meegid.2011.01.015

Ambrose, C.D., Crease, T.J., 2010. Evolution of repeated sequences in the ribosomal DNA intergenic spacer of 32 arthropod species. J. Mol. Evol. 70, 247–259.
Attwood, S.W., Fatih, F.A., Mondal, M.M.H., Alim, M.A., Fadjar, S., Rajapakse, R., Rollinson, D., 2007. A DNA sequence-based study of the *Schistosoma indicum* (Trematoda: Digenea) group: population phylogeny, taxonomy and historical biogeography. Parasitology 134, 2009–2020.
Blair, D., 2006. Ribosomal DNA variation in parasitic flatworms. In: Maule, A. (Ed.), Parasitic Flatworms: Molecular Biology, Biochemistry, Immunology and Control. CABI, pp. 96–123.
Capowski, E.E., Tracy, J.W., 2003. Ribosomal RNA processing and the role of SmMAK16 in ribosome biogenesis in *Schistosoma mansoni*. Mol. Biochem. Parasitol. 132, 67–74.
Collins, C.M., Cunningham, C.O., 2000. Characterization of the *Gyrodactylus salaris* Malmberg, 1957 (Platyhelminthes: Monogenea) ribosomal intergenic spacer (IGS) DNA. Parasitology 121, 555–563.
Gollapudi, R., Revanna, K.V., Hemmerich, C., Schaack, S., Dong, Q., 2008. BOV—a web-based BLAST output visualization tool. BMC Genomics 9, 414.
Hall, T.A., 1999. BioEdit: a user-friendly biological sequence alignment editor and analysis program for Windows 95/98/NT. Nucleic Acids Symp. Series 41, 95–98.
Hillis, D.M., Dixon, M.T., 1991. Ribosomal DNA: molecular evolution and phylogenetic inference. Q. Rev. Biol. 66, 410–453.
Kane, R.A., Rollinson, D., 1998. Comparison of the intergenic spacers and 3′ end regions of the large subunit (28S) ribosomal RNA gene from three species of *Schistosoma*. Parasitology 117, 235–242.
Lafontaine, D.LJ., 2010. A 'garbage can' for ribosomes: how eukaryotes degrade their ribosomes. Trends Biochem. Sci. 35, 267–277.
Li, Y.S., Sleigh, A.C., Ross, A.G., Williams, G.M., Tanner, M., McManus, D.P., 2000. Epidemiology of *Schistosoma japonicum* in China: morbidity and strategies for control in the Dongting Lake region. Int. J. Parasitol. 30, 273–281.
Lockyer, A.E., Olson, P.D., Østergaard, P., Rollinson, D., Johnson, D.A., Attwood, S.W., Southgate, V.R., Horak, P., Snyder, S.D., Le, T.H., Agatsuma, T., McManus, D.P., Carmichael, A.C., Naem, S., Littlewood, D.T.J., 2003. The phylogeny of the Schistosomatidae based on three genes with emphasis on the interrelationships of Schistosoma Weinland, 1858. Parasitology 126, 203–224.
Mateos, M., Markow, T.A., 2005. Ribosomal intergenic spacer (IGS) length variation across the Drosophilinae (Diptera: Drosophilidae). BMC Evol. Biol. 5, 46.
McGarvey, S.T., Zhou, X.N., Willingham 3rd., A.L., Feng, Z., Olveda, R., 1999. The epidemiology and host–parasite relationships of *Schistosoma japonicum* in definitive hosts. Parasitol. Today 15, 214–215.
Morgan, J.A.T., DeJong, R.J., Kazibwe, F., Mkoji, G.M., Loker, E.S., 2003. A newly-identified lineage of *Schistosoma*. Int. J. Parasitol. 33, 977–985.
Moss, T., Stefanovsky, V.Y., 1995. Promotion and regulation of ribosomal transcription in eukaryotes by RNA polymerase I. Prog. Nucleic Acid Res. Mol. Biol. 50, 25–66.
Nolan, M.J., Cribb, T.H., 2005. The use and implications of ribosomal DNA sequencing for the discrimination of digenean species. Adv. Parasitol. 60, 101–163.
Picón, M., Gutell, R.R., Ehrlich, R., Zaha, A., 1996. Characterization of a flatworm ribosomal RNA-encoding gene: promoter sequence and small subunit rRNA secondary structure. Gene 171, 215–220.
Simpson, A.J., Dame, J.B., Lewis, F.A., McCutchan, T.F., 1984. The arrangement of ribosomal RNA genes in *Schistosoma mansoni*: identification of polymorphic structural variants. Eur. J. Biochem. 139, 41–45.
Schistosoma japonicum Genome Sequencing and Functional Analysis Consortium, Zhou, Y., Zheng, H., Liu, F., Hu, W., Wang, Z.Q., Gang, L., Ren, S., 2009. The *Schistosoma japonicum* genome reveals features of host–parasite interplay. Nature 460, 345–351.
Snyder, S.D., Loker, E.S., 2000. Evolutionary relationships among the Schistosomatidae (Platyhelminthes: Digenea) and an Asian origin for *Schistosoma*. J. Parasitol. 86, 283–288.
Zhang, Z., Schwartz, S., Wagner, L., Miller, W., 2000. A greedy algorithm for aligning DNA sequences. J. Comput. Biol. 7, 203–214.
Zhao, G.H., Mo, X.H., Zou, F.C., Li, J., Weng, Y.B., Lin, R.Q., Xia, C.M., Zhu, X.Q., 2009a. Genetic variability among *Schistosoma japonicum* isolates from different endemic regions in China revealed by sequences of three mitochondrial DNA genes. Vet. Parasitol. 162, 67–74.
Zhao, G.H., Li, J., Zou, F.C., Mo, X.H., Yuan, Z.G., Lin, R.Q., Weng, Y.B., Zhu, X.Q., 2009b. ISSR, an effective molecular approach for studying genetic variability among *Schistosoma japonicum* isolates from different epidemic provinces in mainland China. Infect. Genet. Evol. 9, 903–907.
Zhao, G.H., Li, J., Zou, F.C., Liu, W., Mo, X.H., Lin, R.Q., Yuan, Z.G., Weng, Y.B., Song, H.Q., Zhu, X.Q., 2009c. Heterogeneity of class I and class II MHC sequences in *Schistosoma japonicum* from different endemic regions in mainland China. Parasitol. Res. 106, 201–206.
Zhou, X.N., Wang, L.Y., Chen, M.G., Wu, X.H., Jiang, Q.W., Chen, X.Y., Zheng, J., Utzinger, J., 2005. The public health significance and control of schistosomiasis in China – then and now. Acta Trop. 96, 97–105.
Zhou, P., Chen, N., Zhang, R.L., Lin, R.Q., Zhu, X.Q., 2008. Food-borne parasitic zoonoses in China: perspective for control. Trends Parasitol. 24, 190–196.
Zhu, X.Q., D'Amelio, S., Palm, H.W., Paggi, L., George-Nascimento, M., Gasser, R.B., 2002. SSCP-based identification of members within the *Pseudoterranova decipiens* complex (Nematoda: Ascaridoidea: Anisakidae) using genetic markers in the internal transcribed spacers of ribosomal DNA. Parasitology 124, 615–623.

Please cite this article in press as: Zhao, G.-H., et al., The ribosomal intergenic spacer (IGS) region in *Schistosoma japonicum*: Structure and comparisons with related species. Infect. Genet. Evol. (2011), doi:10.1016/j.meegid.2011.01.015

Ashdin Publishing
Journal of Neuroparasitology
Vol. 2 (2011), Article ID N110701, 5 pages
doi:10.4303/jnp/N110701

Case Report

Cerebral Microsporidiosis Caused by *Encephalitozoon cuniculi* Infection in a Young Squirrel Monkey

K. Furuya,[1] H. Sugiyama,[1] M. Ohta,[2] S. Nakamura,[2] Y. Une,[2] and S. Sasaki[3]

[1] *Department of Parasitology, National Institute of Infectious Diseases, 1-23-1 Toyama, Shinjuku-ku, Tokyo 162-8640, Japan*
[2] *Laboratory of Veterinary Pathology, Azabu University, 1-17-71 Fuchinobe, Sagamihara, Kanagawa 229-8501, Japan*
[3] *Kashima Laboratory, Mitsubishi Chemical Medience Corp., 14 Sunayama, Kamisu, Ibaraki 314-0255, Japan*
Address correspondence to K. Furuya, kfuruya@nih.go.jp

Received 7 July 2011; Accepted 19 July 2011

Abstract This is a case report of cerebral microsporidiosis found in a young squirrel monkey (*Saimiri sciureus*) in a colony located in Japan, which probably died of yersiniosis due to *Yersinia pseudotuberculosis* infection. The microsporidia, *Encephalitozoon cuniculi*, was detected in the brain of the yersiniosis-diseased monkey and was further characterized as a genetically unique type of strain III. The agent was microbiologically and genetically undetectable in other organs tested. Gram-positive organisms, which were confirmed immunohistochemically as *Encephalitozoon spp.* including mature spores, were histologically detected in pseudocysts formed inside neurons and in neuropils. Reactions in the surrounding tissue were not observed for most parasitized lesions. Neurons in the brain of younger hosts might provide a site for latent and active infection by *E. cuniculi*.

Keywords *Encephalitozoon cuniculi*; cerebral microsporidiosis; squirrel monkey; genotype; latent infection

Microsporidian *Encephalitozoon cuniculi* infection in squirrel monkeys has been previously reported [14], where many reported cases were histologically diagnosed. Seropositive cases were also found in many squirrel monkeys (*Saimiri sciureus*) in a primate colony in the United States [9] and also in 11 squirrel monkey colonies in Japan [7]. Therefore, there was a considerable interest in clarifying whether seropositive squirrel monkeys truly develop microsporidiosis or *E. cuniculi* infection. We investigated five squirrel monkeys (AZ1, AZ2, AZ3, AZ4 and AZ5) in one of the 11 colonies located in Japan and determined that two squirrel monkeys (AZ1 and AZ2) had evidence of microsporidiosis. In a previous report, we mainly studied animal AZ1 through genetic testing and diagnosed it with disseminated microsporidiosis due to infection by a genetically unique type of *E. cuniculi* strain III [2]. The present report describes animal AZ2 with cerebral microsporidiosis, based on microbiologic, genetic, serologic, and histological investigation, with emphasis on histological results. The remaining three squirrel monkeys (AZ3, AZ4 and AZ5) were also investigated to understand the infection level in each monkey, and sera from another 14 monkeys in the same colony were also used to understand the endemic prevalence within the colony.

In 2005, two squirrel monkeys (AZ1 and AZ2) died of unknown causes in a colony located in Japan. AZ1 was a 10-day-old squirrel monkey and the AZ2 was a young male squirrel monkey with undeveloped canine teeth and immature testes. The 10-day-old animal and the young animal were later diagnosed with disseminated microsporidiosis [2] and yersiniosis due to *Yersinia pseudotuberculosis*, respectively. Major organs (brain, lung, liver, spleen and kidney) were obtained from the two animals at autopsy in addition to those from the AZ3 (a pubescent one with developed canine teeth and penis but with an undeveloped inguinal canal), AZ4 (adult) and AZ5 (adult) that had been bred in the same colony. The AZ3, AZ4 and AZ5 were humanely sacrificed to perform the various tests. Serologic testing was carried out using spore-ELISA (enzyme-linked immunosorbent assay) to determine IgG antibody against the spore wall (SW) and antibody against the polar tube (PT) of the pathogen [8], using two-fold serial dilutions of sera from a total of 19 monkeys in the colony, starting with a dilution of 1:200. Antibody titers were expressed as the reciprocal of each serum endpoint dilution.

Microbiologic tests were performed using homogenized organ specimens, trypsinized, and washed with 0.25% sodium dodecyl sulfate (SDS) solution. SDS-insoluble precipitates were fractionated by density gradient centrifugation with Percoll (Amersham Biosciences, Uppsala) and the resultant sediments (RS) were subjected to light microscopic test using the Fungi-Fluor stain kit (Polysciences, Warrington, PA, USA) and also genetic analysis, as previously described [2]. Genetic analysis was performed using DNA

	Fungi-Fluor test[1]					PCR test[2]					Serologic test[3]	
Animal	Br	Lu	Li	Sp	Ki	Br	Lu	Li	Sp	Ki	anti-SW	anti-PT
AZ1[4]	+	+	+	+	+	+	+	+	+	+	ND	ND
AZ2	+	−	−	−	−	+	−	−	−	−	800	400
AZ3	−	−	−	−	−	−	−	−	−	−	25600	12800
AZ4	−	−	−	−	−	−	−	−	−	−	3200	3200
AZ5	−	−	−	−	−	−	−	−	−	−	3200	1600

[1] Fungi-Fluor test was performed to detect microsporidian spores in specimens from the brain (Br), lung (Lu), liver (Li), spleen (Sp) and Kidney (Ki). The − and + signs show to be negative and positive, respectively.

[2] PCR test was performed to amplify *E. cuniculi* ITS region. As shown in Figure 1, a 403-bp fragment was amplified from the DNA sample from the brain of AZ2.

[3] Serologic test was performed by spore-ELISA to detect Anti-SW and anti-PT IgG antibodies in the sera. The ELISA titer was expressed as the highest antibody dilution. ND: not done.

[4] The results of AZ1 organs are described in detail in reference [2].

Table 1: Results of laboratory tests of organ specimens and serum samples from squirrel monkeys.

samples separated from the RS specimens, as previously described [2]. The polymerase chain reaction (PCR) was performed using primer sets (5′-tcctagtaatagcggctgac-3′; 5′-tttcactcgccgctactcag-3′) for amplification of the internal transcribed spacer (ITS) region, primer sets (5′-gcagttccaggctactac-3′; 5′-aggaactccggatgttcc-3′) for amplification of the polar tube protein (PTP) coding region, and primer sets (5′-actgacaagtaccacatc-3′; 5′-ttggactcacacattagg-3′) for amplification of the spore wall protein 1 (SWP-1) coding region, as previously described [2, 13]. PCR products were further analyzed using direct DNA sequencing.

Histological analysis was performed using formalin-fixed and paraffin-embedded tissue sections of the brain of AZ2. Tissue sections were stained with hematoxylin and eosin (HE), Brown-Hopps, chromotrope and immunohistochemical methods [5, 12]. In the immunohistochemical test, brain tissue sections were affixed to polylysine-coated microscope slides, deparaffinized and treated with L.A.B. solution (Liberate Antibody Binding Solution; Polysciences) to reactivate damaged antigens. Sections were reacted with biotin-conjugated and affinity-purified rabbit anti-*E. cuniculi* antibodies (primary antibody) and biotinylated goat anti-rabbit IgG solution (secondary antibody; Zymed Laboratories, South San Francisco, CA, USA), followed by ready-to-use streptavidin-peroxidase conjugate solution (Zymed Laboratories). Finally, slides were exposed to HistoMark True Blue (KPL, Gaithersburug, MD, USA) stain, as previously described [5].

The ELISA titer of AZ2 serum was determined to be 800 for anti-SW and 400 for anti-PT antibody. On the other hand, anti-SW and anti-PT antibody titers in sera of AZ3, AZ4 and AZ5 were estimated to be 1600-25200. These results are summarized in Table 1. ELISA antibody titers in sera of 13 out of the other 15 monkeys in the same colony ranged from 800 to 51200 for both anti-SW and anti-PT antibodies.

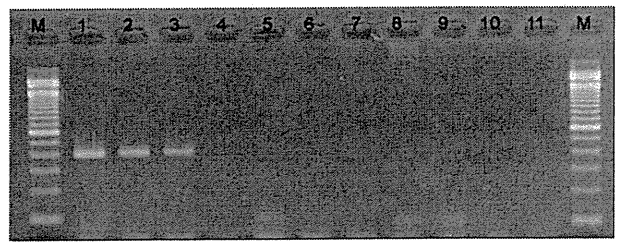

Figure 1: PCR analysis of DNA samples from squirrel monkeys using *E. cuniculi* ITS primers. Lane 1: positive control, a single band at 399 bp for a rabbit *E. cuniculi* DNA sample (strain I); lane 2: a DNA sample from AZ1 brain, which was used as *E. cuniculi* strain III derived from a squirrel monkey; lane 3: AZ2 brain; lane 4: AZ3 brain; lane 5: AZ4 brain; lane 6: AZ5 brain; lanes 7–10: DNA samples from AZ2 organs (lung, liver, spleen and kidney, in left-to-right order); lane 11: water blank; M: a 100-bp DNA ladder marker (Invitrogen, Carlsbad, CA). PCR products were analyzed by 2% agarose gel electrophoresis.

Fungi-Fluor-positive organisms were detected in the brain tissues of AZ2, but not from other organs tested from the same monkey or any organ tested for AZ3, AZ4 and AZ5 (Table 1).

Positive PCR tests targeting ITS, PTP and SWP-1 were detected only from DNA samples extracted from AZ2 brain tissue. ITS PCR amplification revealed a single band of 403 bp on agarose gels (Figure 1). DNA samples from the lung, liver, spleen and kidney were negative for the ITS-PCR. Furthermore, DNA samples from the brain and other organs of AZ3, AZ4 and AZ5 were ITS-PCR negative. These are also summarized in Table 1, in which the results of all the organs of AZ1 are also described for reference. Direct DNA sequencing of the PCR products demonstrated that the *Encephalitozoon* detected in AZ2 brain tissue was

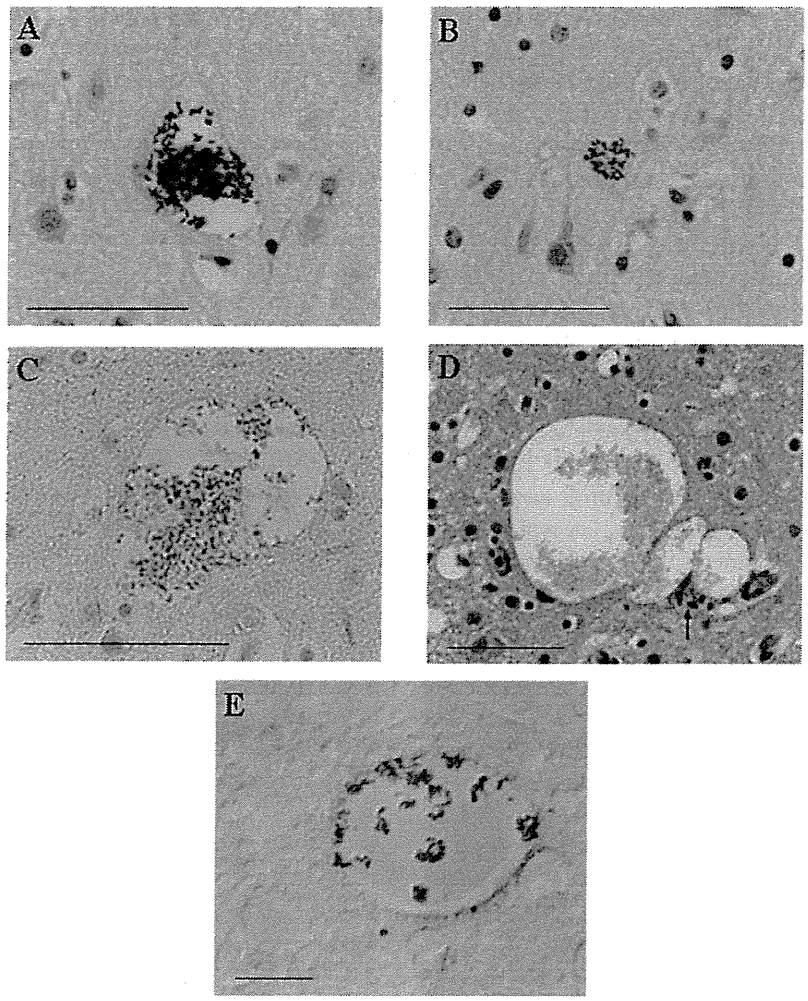

Figure 2: (A) Pseudocyst containing Gram-positive organisms within a neuron in the cerebral cortex (Gram stain, scale bar = 50 μm); (B) Pseudocyst containing Gram-positive organisms in a neuropil in the cerebral cortex (Gram stain, scale bar = 50 μm); (C) Two contiguous pseudocystes containing pink or dark red organisms in the cerebral cortex (chromotrope stain, scale bar = 50 μm); (D) Three contiguous pseudocysts with weak glial reaction (arrow) in the cerebral cortex (HE stain, scale bar = 50 μm); (E) *Encephalitozoon* organisms developing in a pseudocyst in the cerebral cortex (immunostain, scale bar = 10 μm).

E. cuniculi ITS genotype III (i.e. strain III), because of the presence of four repeats of 5′-GTTT-3′. However, further genetic analyses revealed that the detected *Encephalitozoon* had 99% homology with the corresponding region of the *E. cuniculi* genotype II PTP gene (GenBank accession: AF31068) and had the unclassified SWP-1 region (DDBJ accession: AB182699).

Histological evaluation of the brain of AZ2 was conducted on a transverse section of the telencephalon at the level of the thalamus. The histological characteristics of this case were non-suppurative meningoencephalitis, congestion, and fresh hemorrhage. Microscopic lesions in the brain consisted of multifocal microgliosis commonly related to small blood vessels, minimal perivascular cuffing with mononuclear cell infiltration, and partly adventitial cell proliferation. Gram-positive organisms were detected in pseudocysts formed inside neurons (Figure 2A) and in neuropils (Figure 2B). Parasitic organisms in the pseudocysts were also stained pink or dark red by chromotrope staining (Figure 2C). Most pseudocysts had no surrounding tissue reaction. Weak glial reaction was rarely seen around large pseudocysts contiguous to each other (Figure 2D). Perivascular macrophages were shown to have phagocytosed Gram-negative rod-shaped bacteria. Moreover, growth of Gram-negative rod-shaped bacteria free from cells was seen in the lumen of the blood vessels

and in the hemorrhagic focus. Gram-positive organisms were confirmed as *Encephalitozoon spp.* developing inside pseudocysts (Figure 2E), by immunohistochemical staining with biotinylated and affinity-purified rabbit anti-*E. cuniculi* antibody. The HistoMark True Blue substrate deeply stained spores blue that also reacted with specific antibody.

Thus, we detected *Encephalitozoon* spores and DNA in the brain of AZ2 showing a low level of antibody; however, these observations were not found in the brain and other tested organs of AZ3, AZ4 and AZ5 in the same colony despite strongly seropositivity. The genotype of *E. cuniculi* identified in AZ2 was the same as that from the AZ1, which was identified as a genetically unique type of strain III [2]. Serological investigation also indicated the endemicity of *E. cuniculi* in the colony. The results of these analyses suggest that this type of *E. cuniculi* was prevalent among monkeys in the colony, but replication of the agent may have been restricted within newborn or young monkeys. Similar findings have been reported by Zeman and Baskin [14], who studied a series of 22 cases with naturally occurring microsporidiosis in squirrel monkeys from a breeding colony. Most of those monkeys were young, including nine monkeys that were less than four weeks old, and were histologically diagnosed. Furthermore, Anver et al. [1] reported a stillborn, premature male squirrel monkey diagnosed with microsporidiosis as indicated by histologic lesions. Brown et al. [3] described infection in a one-month-old orphan male squirrel monkey that had histologically suspected lesions and Gram-positive organisms in various organs including the brain.

A strong relationship has been proven between *E. cuniculi* genotype and host specificity [4]; for example, strain I was isolated from rabbits, strain II from mice and blue foxes, and strain III from domestic dogs, generally known as the "dog type" [11]. However, *E. cuniculi* strain III has been identified in squirrel monkeys in this and previous studies [2] and does not belong to the "dog type" because it contained a genotype II PTP and an unclassified SWP-1 genotype when being classified according to the procedures performed by Xiao et al. [13]. While such a genomic difference is epidemiologically important for considering the original host of this strain III, it also may have influenced the distribution of the parasite and lesions seen in natural *E. cuniculi* infections of squirrel monkeys in a colony in Japan.

With the exception of perivascular macrophages possessing Gram-negative rod-like organisms, growth of the Gram-negative organisms in the blood vessels and hemorrhagic focus may suggest a postmortem change. Histological observations (Figures 2A and 2B) clearly show that pseudocysts containing Gram-positive *Encephalitozoon* organisms occurred in neurons and in neuropils. However, the host response was not observed in most parasitized lesions, although large pseudocysts rarely accompanied a glial reaction (Figure 2D). Thus, it was likely that the pathogen was reproducing in the absence of a host cell response, although the influence of co-infection by *Y. pseudotuberculosis* on *E. cuniculi* latent infection is unknown. The current investigation and most cases reported in the United States suggest that at younger ages, various organs including the brain provide a favorable environment for latent infection by *E. cuniculi* and for its replication. It seems probable that *E. cuniculi* in an immune-privileged site is capable of remaining undetected in host cells. It has been previously observed that *E. cuniculi* occasionally spontaneously infects primary tissue cultures [10]. Therefore, it would be no surprise that a neuron was one of the target cells for latent infection by this type of strain III, as demonstrated in a study using mice experimentally infected with *Toxoplasma gondii* [6]. The present case is considered a representative example of cerebral microsporidiosis due to *E. cuniculi* strain III infection in young squirrel monkeys, and demonstrates histological features of latent infection.

Acknowledgment We acknowledge Ms. T. Asakura for excellent technical assistance with immunoserologic, immunohistochemical, microbiologic and genetic analyses.

References

[1] M. R. Anver, N. W. King, and R. D. Hunt, *Congenital encephalitozoonosis in a squirrel monkey (Saimiri sciureus)*, Vet Pathol, 9 (1972), 475–480.

[2] T. Asakura, S. Nakamura, M. Ohta, Y. Une, and K. Furuya, *Genetically unique microsporidian Encephalitozoon cuniculi strain type III isolated from squirrel monkeys*, Parasitol Int, 55 (2006), 159–162.

[3] R. J. Brown, D. K. Hinkle, W. P. Trevethan, J. L. Kupper, and A. E. Mckee, *Nosematosis in a squirrel monkey (Saimiri sciureus)*, J Med Primatol, 2 (1973), 114–123.

[4] E. S. Didier and G. T. Bessinger, *Host-parasite relationships in microsporidiosis: animal models and immunology*, in The Microsporidia and Microsporidiosis, M. Wittner and L. M. Weiss, eds., ASM Press, Washington, DC, 1999, 225–257.

[5] K. Furuya, *Spore-forming microsporidian encephalitozoon: current understanding of infection and prevention in Japan*, Jpn J Infect Dis, 62 (2009), 413–422.

[6] T. C. Melzer, H. J. Cranston, L. M. Weiss, and S. K. Halonen, *Host cell preference of Toxoplasma gondii cysts in murine brain: A confocal study*, J Neuroparasitol, 1 (2010), N100505.

[7] M. Ohta, *Epidemiological and pathological studies on encephalitozoon cuniculi infection in squirrel monkeys*, master's thesis, Azabu University, 2007 (in Japanese).

[8] M. Omura, K. Furuya, S. Kudo, W. Sugiura, and H. Azuma, *Detecting immunoglobulin M antibodies against microsporidian Encephalitozoon cuniculi polar tubes in sera from healthy and human immunodeficiency virus-infected persons in Japan*, Clin Vaccine Immunol, 14 (2007), 168–172.

[9] J. A. Shadduck and G. Baskin, *Serologic evidence of Encephalitozoon cuniculi infection in a colony of squirrel monkeys (Saimiri sciureus)*, Lab Anim Sci, 39 (1989), 328–330.

[10] J. A. Shadduck and S. P. Pakes, *Encephalitozoonosis (nosematosis) and toxoplasmosis*, Am J Pathol, 64 (1971), 657–672.

[11] A. Tosoni, M. Nebuloni, A. Ferri, S. Bonetto, S. Antinori, M. Scaglia, et al., *Disseminated microsporidiosis caused by Encephalitozoon cuniculi III (dog type) in an Italian AIDS patient: a retrospective study*, Mod Pathol, 15 (2002), 577–583.
[12] R. Weber, D. A. Schwartz, and P. Deplazes, *Laboratory diagnosis of microsporidiosis*, in The Microsporidia and Microsporidiosis, M. Wittner and L. M. Weiss, eds., ASM Press, Washington, DC, 1999, 315–362.
[13] L. Xiao, L. Li, G. S. Visvesvara, H. Moura, E. S. Didier, and A. A. Lal, *Genotyping Encephalitozoon cuniculi by multilocus analyses of genes with repetitive sequences*, J Clin Microbiol, 39 (2001), 2248–2253.
[14] D. H. Zeman and G. B. Baskin, *Encephalitozoonosis in squirrel monkeys (Samiri sciureus)*, Vet Pathol, 22 (1985), 24–31.

＜国内情報＞

食用として販売されていたサワガニからの肺吸虫メタセルカリアの検出（続報）

食用に販売された淡水産カニを感染源とする肺吸虫症例が続発したことから，食用のサワガニを購入して検査し，ウェステルマン肺吸虫および宮崎肺吸虫のメタセルカリア（人への感染能力を持つ幼虫）を検出した。この検査結果は本誌で報告し[1]，サワガニは食用として販売されていても，肺吸虫感染の原因食品として危険であることを指摘した。しかしながら，食用のサワガニを感染源と疑う肺吸虫症例の報告は，以降も続いている[2,3]。

そこで東京都内で食用のサワガニを購入し，452匹を改めて検査したところ，49匹（11%）からウェステルマン肺吸虫あるいは宮崎肺吸虫のメタセルカリアが検出された（表1）。

サワガニを喫食するのであれば，事前の温度処理が有効と考え，ウェステルマン肺吸虫（2倍体型）陽性のサワガニを用いて，実験的な検討を行った。その結果，加熱（55℃・5分間以上）[4]あるいは冷凍（−18℃・100分間以上）したサワガニ由来のメタセルカリアは，実験動物に投与しても感染しなかった。このような成績も参照し，肺吸虫感染の原因食品となるサワガニについて，積極的な対応を進める必要があると考えられた。

参考文献
1) 杉山　広ら, IASR 29: 284-285, 2008
2) 杉山　広ら, Clin Parasitol 19: 86-88, 2008
3) 高木雄亮ら, 呼吸器誌 47: 249-253, 2009
4) 杉山　広ら, Clin Parasitol 21: 43-45, 2010

国立感染症研究所寄生動物部
杉山　広　森嶋康之　山崎　浩
国立医薬品食品衛生研究所食品衛生管理部
春日文子

表1. 東京都内において食用として販売されていたサワガニからの肺吸虫メタセルカリアの検出状況

購入時期	産地	検査数	陽性数(%)	検出メタセルカリア数	同定結果*
2008.8.	宮崎	5	1 (20)	5	Pm
2008.8.	宮崎	33	0 (0)	0	-
2008.8.	宮崎	41	0 (0)	0	-
2009.5.	宮崎	45	6 (13)	19	Pm+Pw(2n)
2009.5.	佐賀	90	27 (30)	126	Pm
2009.6.	静岡	56	2 (4)	3	Pm
2010.6.	宮崎	67	0 (0)	0	-
2010.9.	宮崎	48	2 (4)	7	Pw(3n)
2010.9.	宮崎	42	6 (14)	68	Pw(3n)
2011.4.	宮崎	25	5 (20)	16	Pw(3n)
合計		452	49 (11)	244	

* Pm：宮崎肺吸虫；Pw(2n)：ウェステルマン肺吸虫（2倍体型）；
Pw(3n)：ウェステルマン肺吸虫（3倍体型）